

# 1 **What Drives Basin Scale Spatial Variability of Snowpack** 2 **Properties in the Front Range of Northern Colorado?**

3  
4 **G. A. Sexstone and S. R. Fassnacht**

5 {ESS-Watershed Science Program, Warner College of Natural Resources, Colorado State  
6 University, Fort Collins, Colorado 80523-1476, USA }

7 Correspondence to: G. A. Sexstone (Graham.Sexstone@colostate.edu)

## 8 9 **Abstract**

10 This study uses a combination of field measurements and Natural Resource Conservation  
11 Service (NRCS) operational snow data to understand the drivers of snow density and snow  
12 water equivalent (SWE) variability at the basin scale (100s to 1000s km<sup>2</sup>). Historic snow  
13 course snowpack density observations were analyzed within a multiple linear regression snow  
14 density model to estimate SWE directly from snow depth measurements. Snow surveys were  
15 completed on or about 01 April 2011 and 2012 and combined with NRCS operational  
16 measurements to investigate the spatial variability of SWE near peak snow accumulation.  
17 Bivariate relations and multiple linear regression models were developed to understand the  
18 relation of snow density and SWE with terrain variables, (derived using a geographic  
19 information system (GIS)). Snow density variability was best explained by day of year, snow  
20 depth, UTM Easting, and elevation. Calculation of SWE directly from snow depth  
21 measurement using the snow density model has strong statistical performance and model  
22 validation suggests the model is transferable to independent data within the bounds of the  
23 original dataset. This pathway of estimating SWE directly from snow depth measurement is  
24 useful when evaluating snowpack properties at the basin scale, where many time consuming  
25 measurements of SWE are often not feasible. A comparison with a previously developed  
26 snow density model shows that calibrating a snow density model to a specific basin can  
27 provide improvement of SWE estimation at this scale, and should be considered for future  
28 basin scale analyses. During both water year (WY) 2011 and 2012, elevation and location  
29 (UTM Easting and/or UTM Northing) were the most important SWE model variables,  
30 suggesting that orographic precipitation and storm track patterns are likely driving basin scale

Deleted: spatial

Deleted: and canopy variables

Deleted: consistent drivers of

1 SWE variability. ~~Terrain~~ curvature ~~was~~ also shown to be ~~an~~ important variable, but to a lesser  
2 extent at the scale of interest.

**Deleted:** Terrain characteristics, such as slope, aspect, and

**Deleted:** , were

**Deleted:** s

## 4 1 Introduction

5 A majority of earth's moving freshwater originates in snow dominated mountainous areas  
6 (Viviroli et al., 2003), with 60 to 75 percent of annual streamflow in the Rocky Mountain  
7 region of the western United States originating from snowmelt (Doesken and Judson, 1996).

8 A comprehensive understanding of the distribution of the seasonal mountain snowpack and  
9 estimation of its snow water equivalent (SWE) is essential to improve hydrologic models used  
10 for forecasting water availability. Additionally, the recent shift towards earlier snowmelt in  
11 regions of the western U.S. (e.g. Stewart, 2009; Clow, 2010) necessitates a more accurate  
12 accounting for future water resources planning. Mountainous landscapes have complex  
13 topography as well as strong and highly variable climatic gradients yielding spatial and  
14 temporal (seasonal and interannual) variability in snowpack properties. Determining the  
15 meteorology and related feedbacks that drive hydrologic processes in these areas is  
16 challenging, ~~as~~ the resolution of available SWE measurements is ~~often~~ much larger than the  
17 scale needed to characterize the correlation length of its spatial variability (Blöschl, 1999),  
18 ~~requiring spatial scaling (Bales et al., 2006).~~

**Deleted:** in such complex terrain

**Deleted:** and requires spatial scaling (Bales et al. 2006). Often

19 Across the western U.S., the Natural Resource Conservation Service (NRCS) SNOWpack  
20 TELEmetry (SNOTEL) and snow course network provide operational snowpack  
21 measurements of snow depth and SWE and thus calculated average density at a daily and  
22 monthly time step, respectively. ~~Hourly SNOTEL data are also available.~~ NRCS operational  
23 stations were established to measure the snowpack for water supply forecasts, yet, they have  
24 been shown to represent SWE only as a point location rather than surrounding area (Molotch  
25 and Bales, 2005). Nonetheless, SNOTEL and snow course sites are the most widely available  
26 and utilized ground based measurements of SWE and relied upon heavily for estimating basin  
27 scale snow distribution.

28 Research on the spatial distribution of snow has emphasized the statistical relation between  
29 snow properties and terrain characteristics, the latter as a surrogate for the driving  
30 meteorology. These studies have used SNOTEL data to interpolate SWE over large basins  
31 (e.g. Fassnacht et al., 2003), as well as ~~manual field~~ snowpack measurements over small  
32 catchments (e.g. Elder et al., 1991). However, few studies have analysed snow's spatial

**Deleted:** field

1 | variability at the basin scale using both operational and field-based measurements.  
2 | Operational measurements can provide regional knowledge on the spatial distribution of snow  
3 | (e.g. Fassnacht et al., 2003), yet cannot accurately characterize the spatial variability of the  
4 | snowpack at the basin scale (Bales et al., 2006). It has been recommended that future  
5 | research should focus on more accurate estimation of SWE at the basin (100s to 1000s km<sup>2</sup>)  
6 | and regional (10,000s to 100,000s km<sup>2</sup>) scale to effectively assess and manage mountain  
7 | water resources (Viviroli et al., 2011). ~~There is need to supplement operational data with~~  
8 | additional field-based snowpack measurements at this scale of interest to evaluate the spatial  
9 | variability of SWE and provide additional ground truth measurements within the scale extent  
10 | of remote sensing observations. At the basin scale, an approach to reducing the sampling  
11 | effort needed for more measurements is to use snow depth as a surrogate for SWE by  
12 | developing a model for snow density, as manual snow density measurements require more  
13 | time and effort than snow depth measurements. Recent studies have attempted to characterize  
14 | the spatiotemporal characteristics of snow density (e.g. Mizukami and Perica, 2008; Fassnacht  
15 | et al., 2010), or to develop reliable methods for modeling snow density and thus estimating  
16 | SWE from snow depth measurements (e.g. Jonas et al., 2009, Sturm et al., 2010).

Deleted: , thus t

17 | The objectives of this research were: (1) to evaluate basin scale snow density variability from  
18 | historic snow course measurements and develop a snow density model specific to our study  
19 | area that can be used to estimate SWE from snow depth measurements; this is a different  
20 | domain and scale than used in previous studies, and (2) to combine operational SNOTEL and  
21 | snow course measurements, as suggested by Dressler et al. (2006), with supporting field-  
22 | based snowpack measurements to evaluate what is driving variability of the snowpack at the  
23 | basin scale.

24

## 25 | 2 Study area and datasets

26 | This study was conducted in the Cache la Poudre basin located in the Front Range of northern  
27 | Colorado and a small portion of southeastern Wyoming (Fig. 1). We focus on the portion of  
28 | this basin that shows persistent snow cover near peak snow accumulation; this region is  
29 | responsible for the majority of hydrologic input to the river system. To define this area, we  
30 | use the Snow Cover Index (SCI) at 50% (Richer et al., 2013), which represents the area that  
31 | was snow covered at least 50% of the time from 2000 – 2010 during early April. The SCI is  
32 | calculated based on the Moderate Resolution Imaging Spectroradiometer (MODIS)/Terra

Deleted: is

Deleted: e

Deleted: because it

1 | eight-day snow cover products. The portion of the basin within the 50% SCI has an area of  
2 | 1493 km<sup>2</sup> and ranges in elevation from 2040 to 4125 m. Spruce-fir (*Picea engelmannii* and  
3 | *Abies lasiocarpa*), lodgepole pine (*Pinus contorta*), and ponderosa pine (*Pinus ponderosa*)  
4 | forests cover a majority of this area, with the alpine community located at the highest  
5 | elevations and the mountain shrub community located at the lowest elevations. Snow is the  
6 | dominant form of precipitation within the basin, and the hydrograph peak is driven by  
7 | snowmelt generally occurring in late May to June. The majority of winter moisture moves  
8 | into this region by pacific frontal storm tracks from the west, southwest, or northwest,  
9 | however, systems moving north from the Gulf of Mexico can also bring substantial snowfall  
10 | to the Front Range of Colorado (Barry, 2008).

11 | The NRCS operational stations located within the study area and in a 15 km buffer around the  
12 | basin were analysed (Fig. 1), yielding a total of 10 SNOTEL stations and 17 snow courses.  
13 | Deadman Hill and Joe Wright, the two long-term SNOTEL stations located within the Cache  
14 | la Poudre basin, have a mean (1980 to 2012) peak SWE of 538 mm and 690 mm, respectively  
15 | (Fig. 2). The lowest snow year recorded was 2002 at Deadman Hill and 2012 at Joe Wright,  
16 | while the maximum snow year was 2011 at both SNOTEL stations. Despite the similar  
17 | elevation of the two stations, historically Joe Wright (3085 m) has a greater accumulation of  
18 | snow than Deadman Hill (3115 m).

19 | Field snow surveys were conducted on and about 01 April 2011 and 2012 within the study  
20 | area. At each field sampling location, snow density ( $\rho_s$ ) and/or snow depth ( $d_s$ ) measurements  
21 | were taken and Universal Transverse Mercator (UTM) geographic coordinates were recorded  
22 | using a Global Positioning System (GPS). Eleven measurement points of snow depth (using a  
23 | snow depth probe to the near cm of depth) were averaged across a one-meter interval in one  
24 | of the four cardinal directions to account for the small scale spatial variability at each,  
25 | sampling location (e.g. López-Moreno et al., 2011). Snow density is a conservative variable  
26 | that varies less spatially than depth (Logan, 1973; Fassnacht et al., 2010), thus, fewer  
27 | snowpack density measurements were made across the study area than depth. Three methods  
28 | of measuring snow density were used at each site. A cylindrical metal can with a diameter of  
29 | 15.3 cm was used to measure snow density if the snowpack was less than 50 cm. A  
30 | cylindrical plastic snow sampling tube with a diameter of 6.6 cm was used to measure snow  
31 | density for snowpacks greater than 50 cm and less than 150 cm. Additionally, a Federal  
32 | Sampler (diameter of 3.77 cm) was used to measure the snow density for snowpacks greater

Deleted: upper

Deleted: that contributes to the canyon mouth (gaged by Colorado Division of Water Resources gaging station Cache la Poudre River at Canyon Mouth)

Deleted: 2729

Deleted: 1591

Deleted: a

1 than 150 cm, but it was also used at some locations shallower than 150 cm. Each of the field-  
2 based surveys included transects of sampling locations with a systematic spacing of  
3 approximately 500 meters (Fig. 1). A total of 28 field sampling locations were monitored on  
4 and about 01 April 2011 and 104 field sampling locations on and about 01 April 2012. The  
5 location of snow survey transects were selected based on accessibility as well as  
6 representation of snow producing regions within the study area. The high elevation areas  
7 located around the Colorado State University Pingree Park Campus, Cameron Pass, and  
8 Deadman Hill were the focus within the Cache la Poudre basin (Fig. 1).

9 The 2011 field-based snow survey was completed over the span of three days (31 March  
10 through 02 April 2011), while the 2012 survey was completed over four days (29 March  
11 through 01 April 2012). Small amounts of precipitation was recorded at SNOTEL stations  
12 within the study area during the 2011 and 2012 survey time period, however the majority of  
13 change to the snowpack during these periods were due to melt, compaction, and/or  
14 metamorphism. Changes in snow depth were accounted for using daily SNOTEL snow depth  
15 measurements to standardize the field-based snow depth measurements to a single date for  
16 each survey. The average change in snow depth among SNOTEL stations was added to our  
17 field-based snow depth measurements outside of the standardized date to adjust for the  
18 change in snow depth over that period. Snow depth measurements from the 2011 survey were  
19 standardized to 02 April, while 2012 measurements were standardized to 31 March.

## 21 **3 Background and Methods**

### 22 **3.1 Snow density model**

23 SWE, in millimeters, is the product of snow depth ( $d_s$ ) measured in meters and snow density  
24 ( $\rho_s$ ) divided by the density of water ( $\rho_w$ ) in kilograms per cubic meter. The seasonal  
25 variability of snow density is largely dictated by time of year, while inter-annual variability  
26 observed at operational sites is typically low (Mizukami and Perica, 2008). However,  
27 previous spatial snow surveys have shown that snow density can exhibit inter-annual  
28 variability, particularly in continental regions (e.g. Balk and Elder, 2000; Jepsen et al., 2012).  
29 Snow density tends to increase gradually throughout the snow season due to crystal  
30 metamorphism, settling, and compaction. Therefore, snow density tends to increase with the  
31 day of year (Mizukami and Perica, 2008) and with increasing snow depth (Pomeroy and Gray,

**Deleted:** multiple

**Deleted:** , with each transect consisting of a number of snowpack sampling locations with a systematic sampling spacing of approximately 500 meters.

**Deleted:** 42

**Deleted:** 21

**Deleted:** Since the range of variability of snow density is more conservative than snow depth and SWE (e.g. Logan, 1973; Fassnacht et al., 2010), estimating density from depth has been shown to provide a reasonable pathway for estimating SWE from a snow depth measurement.

1 1995). Elevation has also been shown to influence snow density, with the effect often being  
2 dependent on day of year (e.g. Jonas et al., 2009). Topography and tree canopy also impact  
3 snow densification, as they can be surrogates for solar radiation. However, large datasets of  
4 snow density are not often representative of varying terrain and canopy conditions, which  
5 limits the ability of these data to represent the variability explained by those variables. Since  
6 the range of variability of snow density is more conservative than snow depth and SWE (e.g.  
7 Logan, 1973; Fassnacht et al., 2010), estimating density from depth has been shown to  
8 provide a reasonable pathway for estimating SWE from a snow depth measurement. Based  
9 on the approaches presented by Jonas et al. (2009) and Sturm et al. (2010) we have evaluated  
10 historic operational snow density data for the Cache la Poudre basin and developed a snow  
11 density model. We acknowledge that the operational snow density data evaluated are not  
12 representative of potential terrain and canopy controls on the variability of snow density at the  
13 basin scale. However, the potential drivers of snow depth, time of year, elevation, and region  
14 are adequately represented. The development of this type of model provides a mechanism for  
15 estimating SWE from snow depth, and also may provide insights into regional tendencies of  
16 snow density variability.

**Deleted:** Therefore, SWE can be computed from measured snow depth by estimating snow density.

**Deleted:** developed a model for snow density that can be used to estimate SWE from snow depth

17 Historical data from 17 NRCS snow courses (1936 to 2010, n = 3637; Fig. 1) were evaluated.  
18 These snow courses range in elevation from 2408 m to 3261 m and are (generally) measured  
19 on or about the first of the month from January through June each year. Snow course  
20 measurements consist of the average of approximately ten measurements that are made with a  
21 Federal Sampler. For the analysis, snow density values greater than 600 kg m<sup>-3</sup> and less than  
22 50 kg m<sup>-3</sup> were omitted. Additionally, due to the limited precision and possibly the lack of  
23 accuracy for snow density measurements in shallow snowpacks, data for snow depth less than  
24 0.13 m and/or SWE less than 50 mm were also omitted. This selection of data resulted in  
25 3262 data records of snow depth, snow density, and SWE, with 10.3% of the original data  
26 being removed.

27 A multiple linear regression model was developed to predict snow density considering snow  
28 depth ( $d_s$ ), Julian day (DOY), elevation ( $z$ ), UTM Easting ( $UTM_e$ ), and UTM Northing  
29 ( $UTM_n$ ) as independent variables. The statistical software R (R Development Core Team,  
30 2012) was used for all statistical analyses. The final independent variables included in the  
31 multiple linear regression model were selected based on an all-subsets regression procedure  
32 (Berk, 1978), which assesses a criterion statistic for every possible combination of

**Deleted:** The seasonal variability of snow density is largely dictated by time of year, while inter-annual variability is minimal (Mizukami and Perica, 2008). Snow density tends to increase gradually throughout the snow season due to crystal metamorphism, settling, and compaction. Therefore, snow density tends to increase with the day of year (Mizukami and Perica, 2008) and with increasing snow depth (Pomeroy and Gray, 1995). Topography and tree canopy also impact snow densification, as they can be surrogates for solar radiation. However, snow courses are often located in flat open areas, limiting the ability of the dataset to represent the variability explained by those variables.¶

1 independent variables. Mallows'  $C_p$  (Mallows, 1973), which assesses the fit of a regression  
2 model and increases a penalty term as the number of predictor variables increases, was used  
3 as a criterion for the all-subsets regression. Additionally, a criterion was set so that all  
4 predictor variables included were required to be statistically significant within the model ( $p <$   
5 0.05). Candidate models that showed the best Mallows'  $C_p$  values were then evaluated using  
6 the Akaike information criterion (AIC) statistic (Akaike, 1974), which is also a measure of the  
7 relative goodness of fit of the statistical model that introduces a penalty for increasing the  
8 number of model parameters. The variance inflation factor (VIF) was used to quantify the  
9 severity of multicollinearity between independent variables. A VIF score greater than 4 may  
10 suggest multicollinearity between variables (Kutner et al., 2005). Model diagnostics were  
11 evaluated using residual plots to check the model assumptions of normality, linearity, and  
12 homoscedasticity and were used to determine if variable transformations were necessary.  
13 Final model selection was based on the results of criterion statistics and model diagnostics  
14 (Kutner et al., 2005). Also, if an effort to ensure our model is physically robust, independent  
15 variables were only included within the model if their coefficients made physical sense.

16 The multiple regression model provides an estimate of snow density for each snow depth  
17 measurement and their product yields an estimate of SWE. To assess the accuracy of the  
18 snow density model, several methods of model evaluation were performed. Calibration was  
19 performed by comparing modeled snow density as well as calculated SWE with observed  
20 values from the original dataset; explained variance was computed. Model validation with  
21 two sets of independent data was also completed to test model transferability to predict  
22 independent data. The two independent datasets included monthly (January through May)  
23 field-based measurements from the 2011 and 2012 snow seasons ( $n = 84$ ), as well as historic  
24 first of the month SNOTEL measurements ( $n = 121$ ) at sites that are not co-located with a  
25 snow course. The monthly field-based snow density measurements not collected about 01  
26 April were only used for model validation within this study. Additionally, a 10-fold cross  
27 validation procedure, which runs 10 iterations of removing a random selection of the dataset  
28 and fitting the regression to the remainder of the data, was used to compare modeled values to  
29 the observed values removed for each iteration. Performance of the final snow density model  
30 was determined from the residuals of both observed snow density as well as calculated SWE  
31 through the calculation of the Nash-Sutcliffe Coefficient of Efficiency (NSCE) and Root  
32 Mean Squared Error (RMSE) performance statistics.

### 1 3.2 Basin scale SWE variability

2 Topographic variables that are thought to potentially drive the spatial distribution of snow at  
3 the scale of interest were derived from a 30 m resolution digital elevation model (DEM) of the  
4 study area. The DEM was downloaded from the USGS National Elevation Dataset (NED)  
5 ([ned.usgs.gov](http://ned.usgs.gov)). A value of the derived terrain variables (spatial data grids) was extracted  
6 for each sampling location based on its corresponding 30 m DEM pixel. A description of the  
7 derivation and importance of each of the spatial data grids is provided below.

**Deleted:** Additionally, canopy density was obtained from the National Land Cover Database (NLCD 2001) (<http://www.mrlc.gov>).

**Deleted:** and canopy

8 Location within the study area is represented by UTM Zone 13N Easting and Northing  
9 coordinates for each operational and field-based sampling location. A 30 m resolution spatial  
10 data grid of UTM Easting and Northing was created for the study area in ArcGIS (ESRI,  
11 2011) by assigning the mean UTM value to each pixel. Spatially continuous coordinates of  
12 UTM Easting and Northing can be correlated with the distribution of snow in various ways  
13 that depend on site location and scale. Previous studies have used distance to a mountain  
14 barrier and distance to ocean or source of moisture (e.g. Fassnacht et al., 2003; López-Moreno  
15 and Nogués-Bravo, 2006), which can also be represented by UTM Easting for the study site  
16 due to its geographic orientation. Furthermore, given the scale of the study, UTM Easting and  
17 Northing represent different regions within the study area that are thought to display different  
18 patterns of snow accumulation and ablation due to the variability of meteorology and storm  
19 tracks.

**Deleted:** field-based and operational

20 Elevation was extracted for each sampling location directly from the 30 m DEM. Snow  
21 accumulation has long been shown to be a function of elevation (e.g. Washichak and  
22 McAndrew, 1967; Dingman, 1981) due to orographic precipitation patterns and the effect of  
23 air temperature (Doesken and Judson, 1996).

24 Slope was derived from the 30 m DEM using the Spatial Analyst tools within ArcGIS to  
25 provide an output spatial data grid with a value of slope (in degrees) for each pixel. The  
26 degree of slope impacts the stability of the snowpack (influencing snow accumulation and  
27 redistribution) and input of solar radiation (influencing melt) (Anderton et al., 2004). We  
28 would expect to see a negative correlation between SWE and terrain slope. Previous studies  
29 have successfully used slope angle as an explanatory variable within statistical models  
30 describing the distribution of snow (e.g. Erxleben et al., 2002).

**Deleted:** ; Winstral et al., 2002

31 Aspect (in degrees) was also derived from the 30 m DEM using the Spatial Analyst tools  
32 within ArcGIS. Aspect can be problematic as an independent variable due to its continuous

1 range of 0 to 360 degrees, thus normalizing this variable is necessary. Degrees of northness  
2 and eastness were calculated to normalize the aspect variable (Fassnacht et al., 2001;  
3 Fassnacht et al., 2012). Degree of northness is the product of the cosine of aspect and the sine  
4 of slope (Molotch et al. 2005), while degree of eastness is the product of the sine of aspect  
5 and the sine of slope. Northness is a measure of the degree that terrain is north facing,  
6 therefore we would expect SWE to show a positive correlation with northness as snow tends  
7 to be more persistent on north facing slopes. Similarly, eastness is a measure of the degree  
8 that terrain is east facing. Within our study area, we expect eastness to show a positive  
9 correlation with SWE as east facing slopes are most often the leeward side of dominant west  
10 winds and can receive snow loading from windward slopes. Exposure of slope aspect  
11 controls solar radiation input, which influences snowpack stability, densification, and ablation  
12 (McClung and Schaerer, 2006).

13 Solar radiation was derived using the Area Solar Radiation tool in ArcGIS, which calculates  
14 incoming solar radiation across a DEM surface for a specified time interval. Given the  
15 latitude of the study area, the average clear sky solar radiation (in  $W_m^{-2}$ ) from November 15  
16 through March 30 was calculated for each pixel. Cumulative incoming solar radiation is  
17 calculated based on solar zenith angle and terrain shading, and does not consider the influence  
18 of forest canopy. Previous studies have successfully used solar radiation spatial data grids  
19 derived by similar methods within statistical models describing the distribution of snow (e.g.  
20 Elder et al., 1998; Anderton et al., 2004; Erickson et al., 2005).

21 Terrain curvature was derived from the 30 m DEM using the Spatial Analyst tools within  
22 ArcGIS to provide an output spatial data grid with a value of curvature for each pixel. Terrain  
23 curvature is defined as the second derivative of the surface (Kimerling et al., 2011). Terrain  
24 curvature, heron referred to as curvature, is a combination of profile and planform curvature.  
25 This variable represents the local relief of terrain (i.e. concavity or convexity) in all directions,  
26 which, in terms of snow accumulation, primarily accounts for wind drifting from high  
27 exposure areas with steep slopes to low lying gullies (Blöschl et al., 1991; Lapen and Martz,  
28 1996). Curvature was calculated using both 30 m DEM resolution (90 m footprint) and 100  
29 m DEM resolution (300 m footprint) and will be refered to as curvature 30 and curvature 100,  
30 respectively. Negative curvature values generally represent concave surfaces, thus we expect  
31 curvature and SWE to show a negative correlation due to local snow loading within concave  
32 positioned areas.

Deleted: cumulative

Deleted: H/

Deleted: C

Deleted: the direction of maximum slope

1 Maximum upwind slope (Winstral et al., 2002) is a terrain-based variable that has been shown  
2 to account for redistribution of snow by wind, which is especially important in alpine areas.  
3 However, this variable requires the knowledge of predominant wind direction to account for  
4 upwind terrain features, which is not measured across a basin scale, requiring a modeling  
5 approach (e.g. Liston and Sturm 1998), thus it was not used in this study.

6 Canopy cover is a categorical measurement that was made in the field during manual snow  
7 surveys. The presence of any canopy above the sampling location was assigned a value of  
8 one, while sampling locations with no canopy or open was assigned a zero. We expect  
9 canopy cover to show a negative correlation with SWE. Canopy density can influence how  
10 snow is distributed across space as it is directly related to the amount of snow that is  
11 intercepted in the tree canopy. Snow sublimation from snow intercepted within the forest  
12 canopy is a major component of the overall water balance (Pomeroy and Gray, 1995; Montesi  
13 et al. 2004).

14 Multiple linear regression was used to model 02 April 2011 and 31 March 2012 SWE based  
15 on its relation with independent physiographic variables identified above. A detailed  
16 description of the multiple linear regression methodology is provided above. Multiple linear  
17 regression models were developed using both operational and field snowpack measurements  
18 and also operational measurements only. At this scale of interest, operational data are  
19 commonly the only snowpack data available, thus it was useful to compare the results from  
20 operational data only to those results obtained from using operational data and additional  
21 field-based measurements. The following notation will be used in this study:  $model_{O+F}$  will  
22 refer to the multiple regression model using both operational and field snow measurements  
23 and  $model_O$  will refer to the multiple regression model using only operational snow  
24 measurements. A total of four regression models were developed:  $model_{O+F11}$  (operational  
25 and field data from 2011),  $model_{O11}$  (operational data from 2011),  $model_{O+F12}$  (operational and  
26 field data from 2012), and  $model_{O12}$  (operational data from 2012).

27

## 28 4 Results

### 29 4.1 Snow density model

30 The pairwise relations between snow depth, snow density, and SWE from the historic snow  
31 course records are presented in Fig. 3. A strong correlation exists between snow depth and

**Deleted:** ¶

Canopy density is derived from Landsat Enhanced Thematic Mapper+ (ETM+) circa 2001 satellite data and DEM derivatives (Homer et al., 2007). The canopy density spatial data grid provides an estimated percentage of canopy cover for each pixel at a 30 m resolution.

**Deleted:** field and operational

**Deleted:** field and operational

**Deleted:** field and operational

**Deleted:** field and operational

1 SWE, which is best fit as a power function (Fig. 3a). There is considerable scatter about the  
2 linear fit for snow density versus snow depth (Fig. 3b), which suggests that additional  
3 variables should be included to describe the variability of snow density. Snowpack relations  
4 shown here are similar to those found in previous studies (e.g. Jonas et al., 2009; Sturm et al.,  
5 2010).

6 The mean snow density from the snow course dataset is  $287 \text{ kg m}^{-3}$  with a standard deviation  
7 of  $64.8 \text{ kg m}^{-3}$ . SWE and snow depth have a greater coefficient of variation (0.65, 0.50,  
8 respectively) compared to snow density (0.23). Snow density is most highly correlated with  
9 Julian day, and also shows a positive correlation with snow depth and elevation and negative  
10 correlation with UTM Easting (Table 1). The location dependent correlation with snow  
11 density has been shown in previous studies (e.g. Mizukami and Percia, 2008), however, is  
12 often based on a larger domain and representative of difference climatology. The correlation  
13 of UTM Easting and snow density found from this basin scale dataset may be representing the  
14 impact of the distance to a mountain barrier or storm track patterns on snow density patterns.

Deleted: standard deviation

Deleted: 178 mm

Deleted: 0.46 m

Deleted: their mean (275 mm, 0.92 m, respectively) than

Deleted: strong

15 The final snow density model takes the following form

$$16 \quad \rho_s = 844 + 1.06DOY + 26.1d_s^{0.5} + 4.0 \times 10^{-2}z - 1.78 \times 10^{-3}UTM_e \quad (1)$$

17 where  $\rho_s$  is snow density, DOY is Julian day,  $d_s$  is snow depth,  $z$  is elevation, and  $UTM_e$  is  
18 UTM Easting. A square root transformation of snow depth was made to satisfy model  
19 assumptions. All variables included were shown to have statistical significance ( $p < 0.05$ ).

20 The variance inflation factor (VIF) is less than 2.2 for each variable within the final model,  
21 suggesting that multicollinearity between independent variables is not observed. The  
22 residuals of the regression model are normally distributed and do not violate the underlying  
23 assumptions of the regression (normality, linearity, homoscedasticity).

Deleted: , thus no data transformations were necessary

24 The calibrated model underestimated more dense snowpacks and overestimated less dense  
25 snowpacks, while calculated SWE showed generally unbiased residuals that tended to slightly  
26 increase with increasing observed SWE (Fig. 4). Performance statistics calculated from the  
27 residuals of calibration with the original dataset showed that predicted snow density explained  
28 51% of the total variance in the data with a RMSE of  $45.4 \text{ kg m}^{-3}$ , yet, calculated SWE was  
29 able to explain 94% of the variance in the data and had a RMSE of  $44.2 \text{ mm}$  (Table 1).

Deleted: 3

30 Various methods of model evaluation were performed to test the utility of the regression  
31 model, including 10-fold cross validation, that all showed similar trends (Fig. 4) and

1 comparable error estimates (Table 1) to model calibration. As expected, a minor increase in  
2 error estimation was observed for model validation with independent data, yet the minimal  
3 increase in error shows that the regression model should be transferable to independent data  
4 within the bounds of the original dataset. Thus, we used the snow density model to calculate  
5 SWE for WY 2011 and WY 2012 field-based snow depth measurements.

## 6 4.2 Basin scale SWE variability

7 A total of 51 and 127 snowpack measurements (both operational and field-based) were  
8 analysed from the 02 April 2011 (WY 2011) and 31 March 2012 (WY 2012) snow surveys,  
9 respectively (Fig. 1). The mean SWE and snow depth from WY 2011 were greater than WY  
10 2012, yet the mean snow density and standard deviation of snow density was shown to be  
11 consistent among both years (Table 2). The WY 2011 was the maximum snow year on record  
12 within the study area, while WY 2012 was one of the lowest snow years on record (Fig. 2);  
13 thus WY 2011 snowpack measurements were shown to have a higher mean SWE and snow  
14 depth, but also had a greater range of variability than that of WY 2012 (Table 2). From the  
15 average SWE among SNOTEL stations within the study area, the April 1st snow survey  
16 occurred before peak SWE in 2011, however, occurred slightly after peak SWE before  
17 substantial melt had occurred in 2012. Analysis of the April 1st snowpack from these two  
18 water years allows for the comparison between the two extreme snow years (maximum and  
19 minimum) as well as between two different stages of the niveograph (before and just after  
20 peak SWE).

21 In order to evaluate whether the physiographic variables that were sampled in this study are  
22 representative of their basin scale distributions, we have made comparisons between the  
23 values associated with the sampling locations compared to the values across the study area.  
24 Terrain variables derived within GIS at each of the snowpack measurement locations have  
25 similar averages when compared to the 50% Snow Cover Index (SCI) (Richer et al., 2013)  
26 (Fig. 1), for both 2011 and 2012. Histograms of relative frequency (Fig. 5) show that the  
27 distribution of terrain variables sampled in 2011 and 2012 is similar to the 50% SCI area  
28 distribution of these variables, suggesting that the snowpack measurement locations sampled  
29 during WY 2011 and WY 2012 are representative of the variability of physiography among  
30 the entire study area. The range of values of terrain variables observed at operational stations  
31 tended to be smaller than the field-based station ranges (Fig. 5), which also suggests, the  
32 combination of operational and field-based measurements are more representative of the basin

Deleted: field-based and operational

Deleted: least snowy years

Deleted: during accumulation and melt

Deleted: and canopy

Deleted: and canopy

Deleted: and canopy

Deleted: field-based and operational

1 than the operational measurements alone. A formal Kolmogorov-Smirnov test (K-S test) for  
2 equality of distributions between a random sample ( $n = 244$ ) of the continuous terrain  
3 variables within the 50% SCI area of the basin versus the variables associated with each  
4 WY's sampling locations was completed. The K-S test shows that during both years the  
5 difference between the two samples for curvature, eastness, and canopy density is not  
6 significant enough (95% significant level) to say they have a different distribution. However,  
7 a significant difference between the distributions of elevation, slope, northness, and solar  
8 radiation was observed for both years. The difference in elevation is obvious since field data  
9 are located more at higher elevations than the entire domain (Fig. 5a), and the operational data  
10 tend to be located in a small elevation zone (Fassnacht et al., 2012). Northness is highly  
11 correlated to solar radiation, and both are related to slope so the significance difference for  
12 each of these variables is partly based on their correlation. For avalanche safety purposes,  
13 manual measurements are usually on slopes less than 35 degrees, so steeper slopes can be  
14 underrepresented.

Deleted: and canopy

Deleted: the WY 2011 and WY 2012

Deleted: measurement

15 Snowpack variables were shown to have a strong correlation with each other, with SWE and  
16 snow depth showing the strongest relation (consistent with the historic snow course dataset),  
17 while also showing to be highly correlated with elevation (Table 3). Bivariate relations  
18 showed SWE increased with increasing elevation, with the steepness of this slope being  
19 greater in WY 2011 than 2012. The strength of the correlation between SWE and elevation  
20 for WY 2011 ( $r = 0.75$ ) and WY 2012 ( $r = 0.68$ ) suggests that elevation is the most important  
21 physiographic variable for driving the distribution of SWE across the study domain, which is  
22 consistent with previous findings from studies evaluating SWE at the basin scale (e.g.  
23 Fassnacht et al., 2003; Jost et al., 2007; Harshburger et al., 2010). As UTM Northing  
24 increases, SWE decreases in WY 2011, suggesting northern regions of the study area receive  
25 less snow than southern regions (as suggested by James Meiman, pers. comm., 2010), yet this  
26 trend was not apparent in the low snow year of 2012. Our sample size is only two years,  
27 therefore additional basin scale data are needed to evaluate snow distributions in relation to  
28 UTM Northing, however, historic trends observed from the SNOTEL data suggest that lower  
29 snow amounts in the northern parts of the study area (similar to WY2011) may be more  
30 common (Fig. 2). A greater accumulation of snow in southern regions of the study area could  
31 be related to an upwind elevation gradient, with high peaks of Rocky Mountain National Park  
32 located in the southern portion of the study area, or due to the possibility of a dominant storm  
33 track that preferentially precipitates in southern regions before moving northward. SWE also

Deleted: 7

Deleted: The apparent

1 decreased with increasing UTM Easting, which corresponds with both the effect of  
2 orographic precipitation within the study area (the continental divide is located on the western  
3 border of the study area), and also lower elevation regions receiving less snow than higher  
4 elevation regions. The other physiographic variables that are known to influence snow  
5 accumulation (e.g. forest cover, aspect, and slope) did not exhibit a strong bivariate  
6 correlations with SWE; however, they may still be important in explaining variability of the  
7 datasets once the trends of elevation and UTM coordinates have been removed. The partial  
8 correlations between SWE and terrain/canopy variables (when the correlation effect of  
9 elevation, UTM Easting, and UTM Northing has been removed), shows that curvature  
10 becomes a more important variable when the other trends are removed (Table 4).

Deleted: canopy

11 Multiple linear regression was used to model SWE for 02 April 2011 and 31 March 2012 with  
12 the operational and field-based snowpack dataset (model<sub>O+F</sub>) and the operational snowpack  
13 dataset only (model<sub>O</sub>) (Fig. 6). The final independent variables used within each model, beta  
14 coefficient values, and a summary of model performance statistics is provided in Table 5, and  
15 Fig. 6. To satisfy the assumptions of the regression model and improve overall model  
16 performance, a square root transformation was made to SWE (dependent variable) and slope  
17 (independent variable) for model<sub>O+F11</sub>, which explains 88% of the total variance with an  
18 RMSE of 85.6 mm (all RMSE values were calculated after transformed values have been  
19 converted back). Model<sub>O+F12</sub> (no data transformations) explained 56% of the total variance  
20 and showed an RMSE of 71.5 mm. The operational models were evaluated against observed  
21 values from the entire operational and field dataset. The WY 2011 operational model  
22 (model<sub>O11</sub>) explains 84% of the total variance of the data with an RMSE of 110.1 mm and  
23 includes a square root transformation of SWE. Lastly, model<sub>O12</sub> explains 51% of the total  
24 variance with a RMSE of 75.6 mm. The VIF is less than 1.4 for each variable within all four  
25 of the multiple regression models, suggesting that multicollinearity between independent  
26 variables is not observed. Also, the residuals of each regression model do not violate the  
27 underlying assumptions of the regression (normality, linearity, homoscedasticity).

Deleted: field-based and operational

Deleted: calibration

Deleted: 4

Deleted: 4

Deleted: 95.9

Deleted: 0

Deleted: 6.2

Deleted: 90

Deleted: 72.7

Deleted: 83

Deleted: 46.1

Deleted: and includes a natural log transform of slope

Deleted: 5

28 A comparison of the standardized error estimation between WY 2011 and WY 2012 models  
29 shows that the model<sub>O+F11</sub> has a lower standardized typical magnitude of error (standardized  
30 RMSE) than model<sub>O+F12</sub>, and describes more of the variance in the data ( $R^2$ ) (Table 5).  
31 Similarly, model<sub>O11</sub> has a lower standardized RMSE and greater  $R^2$  value than model<sub>O12</sub>, but  
32 the difference between these two models is less (Table 5). The difference among these

Deleted: 4

Deleted: 4

1 performance statistics can partially be explained by the nature of each snow year (WY 2011  
 2 was the maximum snow year and WY 2012 was amongst the lowest) and sampling scheme.  
 3 WY 2011 showed much more variation in snow amounts than WY 2012, which could explain  
 4 the difference in the RMSE. Additionally, the greater number of measurement locations (n =  
 5 127) in WY 2012 compared to WY 2011 (n = 51) could further explain the difference in R<sup>2</sup>  
 6 between model<sub>O+F11</sub> and model<sub>O+F12</sub>. Given this difference in field-based sampling locations,  
 7 a reduced model<sub>O+F</sub> for WY 2012 was developed including only WY 2012 field-based  
 8 measurement locations that were co-located with WY 2011 measurement locations (n = 42).  
 9 The reduced model included UTM Northing, elevation, and curvature 30, as independent  
 10 variables and explained 70% of the total variance with a standardized RMSE of 30% (Fig. 6).  
 11 The reduced model shows more favourable results than the full model (model<sub>O+F12</sub>),  
 12 suggesting that fewer data points may be the reason for the stronger performance of the WY  
 13 2011 models. However, the reduced model also explained less of the variance in the data than  
 14 model<sub>O+F11</sub>, which suggests that the superior performance of the 2011 models could be due to  
 15 the greater range of observed variability in the data.

**Deleted:** UTM Easting,  
**Deleted:** eastness,  
**Deleted:** northness  
**Deleted:** 67  
**Deleted:** 2  
**Deleted:** se results  
**Deleted:** an improvement from

**Deleted:** increasing the model's ability to describe the variance of the data.  
**Deleted:** Also, the reduced model showed a lower R<sup>2</sup> value than model<sub>O+F11</sub> which suggests that the model performs better for the 2011 snow year due to the greater range of observed variability in the data.

## 17 5 Discussion

18 The snow density model developed across the study area performed relatively well in  
 19 modeling SWE from independent snow depth measurements. Predicted SWE RMSE ranged  
 20 from 44 mm (calibration data) to 70 mm (independent field validation data). Eighty percent  
 21 of all residual values (n = 2613) fell within ± 50 mm. The variance of the model residuals  
 22 were on average within 12.8% of the observed values. Within site variability of SWE has  
 23 been conservatively estimated to be 15 to 25% (Jonas et al., 2009), which suggests that the  
 24 error observed from the model is within the natural range of SWE variability at a site  
 25 (Fassnacht et al., 2008). The small range of error suggests that estimating SWE from snow  
 26 depth measurements through a snow density model works due to the conservative nature of  
 27 snow density; 52% of snow density data values ranged from 250 to 350 kg m<sup>-3</sup>.

**Deleted:** 66  
**Deleted:** Only 0.26% (n = 11) of the validation data showed a residual value outside of one standard deviation of SWE from the original dataset (178 mm). Additionally, 80%  
**Deleted:** 768

28 Using historical operational measurements for development of a basin scale snow density  
 29 model has implications for future field-based basin scale sampling campaigns, suggesting a  
 30 sampling scheme dominated by snow depth measurements may be successful for evaluating  
 31 basin scale SWE variability. The strength and utility of the model developed here is its ability  
 32 to estimate SWE from the most easily measured variable snow depth. Across basin scales,

**Deleted:** regional based

1 | efforts are being made to estimate snow depth using satellite based lidar data, such as ICESat  
2 | (Jasinski et al., 2012). This can improve snowpack estimates across varying domains of  
3 | interest. This method is especially useful for field-based snow surveys at the basin scale, in  
4 | which many snowpack measurements are required, and the assumption of a constant snow  
5 | density across the study area is not valid (López-Moreno et al., 2012).

6 | The snow density model is simple to develop and implement and an effective tool for  
7 | obtaining estimates of SWE from snow depth measurements across basin scale domains. The  
8 | model is however constricted to its spatial domain, range of physiographic inputs, as well as  
9 | temporal coverage, thus, may not be applicable to areas outside of the study area, for  
10 | elevations that are lower than 2408 m or higher than 3261 m, or for snow depths shallower  
11 | than 0.20 m or deeper than 2.52 m.

12 | Given that our snow density model was calibrated specifically for the Cache la Poudre basin,  
13 | it is useful to compare its performance to similar snow density models that have been  
14 | developed from historic data for different domains. Jonas et al. (2009) developed a set of  
15 | regression equations to model snow density using snow depth, day of year, elevation, and  
16 | region for the Swiss Alps, while Sturm et al. (2010) employed a statistical method based on  
17 | Bayesian analysis for the United States, Canada, and Switzerland using snow depth, day of  
18 | year, and climate class. These previous studies and our research show that snow density is a  
19 | conservative variable that varies spatially much less than snow depth and SWE, however the  
20 | previous studies used spatial domains that are orders of magnitude larger than what has been  
21 | presented here, with the current data being at a finer resolution. We have applied the snow  
22 | density alpine model developed by Sturm et al. (2010) to our dataset and directly compared  
23 | the results to those of our snow density model, given their model was developed for global  
24 | applications and data from the western U.S. were used within model development. We did  
25 | not however test the model developed by Jonas et al. (2009), as it was developed specifically  
26 | for Switzerland and requires regional and elevational parameters that are specific to this area,  
27 | and was not developed for use in other areas. The Sturm et al. (2010) alpine model performed  
28 | well when applied to the dataset from this study, showing a snow density RMSE of 58.1 kg  
29 | m<sup>-3</sup> and RMSE of 53.4 mm when used to calculate SWE. Also, the variance described in the  
30 | SWE dataset from this study by the Sturm et al. (2010) model showed a similar strong  
31 | performance (NSCE = 0.91) as our model. However, the model developed in this study out  
32 | performed the Sturm et al. (2010) model, showing an improvement in RMSE for snow density

**Deleted:** The snow course data were collected on or about the 1st of the month from January through June, and thus the model may be less suitable for mid-month days, and may not be useful before January 1st or after June 1st.¶

**Deleted:** S

**Deleted:** . T

1 and SWE by 22% and 17%, respectively. Also, our model showed an improvement of field  
2 validation RMSE by 9% for snow density and 7% for SWE. This shows that calibrating a  
3 snow density model to a specific basin of interest can improve estimates of SWE from snow  
4 depth from models developed from larger domains and should be considered for future basin  
5 scale assessments of SWE.

**Deleted:** While there are differences in the modeled scale, favorable results have been observed in each approach, suggesting this method is applicable for basin wide, regional, and global scales.

6 Despite WY 2011 being a maximum snow year and WY 2012 being a minimum snow year,  
7 the variables driving each SWE regression were similar and included elevation, location  
8 within the basin (UTM Easting and/or UTM Northing), and curvature. The inclusion of  
9 elevation and geographic location within each regression as well as the strong bivariate  
10 correlations of these variables with SWE indicates that they may be consistent drivers of the  
11 spatial variability of SWE at the basin scale, representing how orographic precipitation and  
12 storm track patterns play a strong role in basin scale SWE distribution. Additionally, the  
13 inclusion of terrain curvature within each model suggests that terrain position is also  
14 important at this scale. The importance of solar radiation on the distribution of the snowpack  
15 has been highlighted by previous studies conducted in alpine areas (e.g. Erikson et al. 2005),  
16 however solar radiation was not shown to be important in this study. This is likely because  
17 the clear sky solar radiation does not take into the account shading from tree canopy, therefore  
18 may not represent the impact of solar radiation across the basin scale. Also, although the  
19 canopy cover variable did show the negative correlation with SWE as expected, this  
20 correlation was relatively weak, thus the categorical canopy cover variable we use here is  
21 likely not adequate. There is a need for a finer resolution canopy dataset for basin scale  
22 analyses, as the 30 m resolution National Land Cover Database (NLCD 2001) canopy density  
23 data is not adequate; this dataset often shows SNOTEL stations as having high canopy density  
24 values despite their location within small forest openings. Given that studies (e.g. Fassnacht  
25 et al., 2012) have shown the spatial variability of snow accumulation to be described by  
26 different physiographic variables from year to year, additional years of data collection at the  
27 basin scale are needed for more complete evaluation.

**Deleted:** a variable related to slope, aspect, and/or

**Deleted:** a

**Deleted:** variable (slope, aspect, and/or

**Deleted:** )

**Deleted:** characteristics are

**Deleted:** , but to a lesser degree,

28 Comparison of the error between model<sub>O+F</sub> and model<sub>O</sub> for WY 2011 and WY 2012 shows  
29 that model<sub>O+F</sub> has superior performance statistics for both years (Table 5). Model<sub>O+F</sub> showed  
30 a 22% and 5% improvement in RMSE from model<sub>O</sub> in 2011 and 2012, respectively.  
31 However, model<sub>O11</sub> and model<sub>O12</sub> showed a fairly strong performance with similar predictor  
32 variables as the operational plus field models. The operational regression models may not be

**Deleted:** .

**Deleted:** However, g

**Deleted:** various

**Deleted:** Erickson et al., 2005;

**Deleted:** 4

**Deleted:** M

**Deleted:** similar

**Deleted:** to previous research using operational data at a comparable scale (e.g. Harshburger et al. 2010).

**Deleted:** his strong performance of t

**Deleted:** , however,

1 representing the study area, as SNOTEL measurements have been shown to represent point  
2 locations rather than surrounding areas (Molotch and Bales, 2005) often having more snow  
3 (Daly et al., 2000), and tend to be located in areas with similar physiographic features (flat  
4 and open canopy areas located near tree line).

5 The spatial dataset of field-based snowpack measurements in this study is at a scale similar to  
6 remote sensing observations and modeling applications; these data and the approaches of  
7 empirical modeling (e.g. multiple linear regression) for characterizing the distribution of SWE  
8 at the basin scale can be used in those contexts for validation. For instance, the observed  
9 patterns of SWE variability within this study, showing to be largely driven by elevation and  
10 geographic location, could be compared to the patterns of variability observed within a  
11 physically based snow evolution model. The comparisons of the statistical relation of the  
12 snowpack with terrain based variables and physically based snow evolution modeling can  
13 provide insight for basin scale SWE distribution estimations.

14 There are limitations to this study that must be acknowledged. The representivity of snow  
15 measurements of their surroundings is an important issue often raised in snow hydrology  
16 studies (e.g. Molotch and Bales, 2005). Although our field-based measurements attempted to  
17 account for the fine scale variability by taking 11 measurement points at each sampling  
18 location, it is possible these sampling locations could have fallen on the edge of a 30 m  
19 resolution GIS pixel and not accurately sampled associated terrain variables. The SNOTEL  
20 station snow pillows have been shown to not represent their surroundings which could have  
21 caused further inaccuracies of the DEM derived variables at each of these sites. The use of  
22 multiple linear regression to model non-linear processes for the SWE models developed  
23 within this study is another important limitation. Limitations in this approach have been  
24 presented in previous studies (Elder et al. 1995), however, we do believe that multiple linear  
25 regression was appropriate given the goals of our study. We would have ideally used binary  
26 regression trees (e.g. Elder et al. 1998) to develop the SWE models, but these decision tree  
27 models require larger datasets than available in this study to provide meaningful results.  
28 Given the main goal of the SWE models was use as a tool to evaluate the importance of  
29 individual variables rather than use strictly within a predictive framework, the multiple linear  
30 regression models provide simplicity of the interpretation of model coefficients. Finally, our  
31 field sampling strategy (non-uniform, non-random spacing, and clustered pattern), which is a  
32 different spacing than operational data, may have influenced regression results. Given the

1 extent of the study area evaluated (1493 km<sup>2</sup>), it was necessary to employ this transect based  
2 strategy because of the formidable challenge of accessing these areas throughout the basin on  
3 skis. Each sampling transect with 500 m spacing of sampling locations were generally  
4 around four kilometres in length and were generally located along an elevational gradient  
5 with varying terrain, providing a range of snow conditions to be sampled (Figure 1). Further  
6 evaluation of each of the individual sampling clusters shows that elevation and location have  
7 the strongest correlation with SWE, suggesting the 500 m spacing of the field-based sampling  
8 locations is likely large enough to represent our scale of interest. A plot of UTM Easting and  
9 UTM Northing versus SWE (Figure 7) shows clear regional trends of the distribution of SWE  
10 across the study area. The importance of the UTM coordinates in describing the SWE  
11 distribution is likely not being affected by the sampling clusters, as these same trends were  
12 observed from the operational data (model<sub>o</sub>). Future snow field campaigns at the basin scale  
13 should take strong consideration of the best sampling strategy suited for the challenges of  
14 covering the basin scale.

## 16 6 Conclusions

17 We have used a combination of operational and field-based snow measurements to evaluate  
18 snowpack properties across the basin scale. This research was motivated by the need for  
19 additional ground truth snowpack observations at a scale that coincides with that of remote  
20 sensing observations and is especially pertinent to water resources forecasting.

21 A method for modeling snow density across the Cache la Poudre basin from historical snow  
22 course measurements was employed for estimating SWE from snow depth. The independent  
23 variables of snow depth, day of year, elevation, and UTM Easting were used in a multiple  
24 linear regression model to estimate snow density. Statistics showed strong performance of  
25 SWE calculated from snow depth observations using the snow density model, and model  
26 validation suggests the model is transferable to independent data within the bounds of the  
27 original dataset. The methods here provide a pathway for estimating SWE from snow depth  
28 measurements, which is especially useful when evaluating snowpack properties at the basin  
29 scale, where time consuming field-based measurements of SWE are often not feasible.

30 The spatial variability of SWE within the Cache la Poudre basin was analysed using  
31 operational and field-based snowpack measurements. Bivariate and partial correlations of  
32 SWE<sub>v</sub> with terrain and canopy variables show that elevation, UTM Easting<sub>v</sub>, UTM Northing<sub>v</sub>,

Deleted: field-based and operational

Deleted: field-based and operational

Deleted: relations

Deleted: and snow depth

Deleted: and

1 | and curvature are most correlated with SWE, and thus are drivers of spatial variability at this  
2 | scale. Multiple linear regression models were developed for WY 2011 and WY 2012 using  
3 | both a combined dataset of operational and field-based measurements ( $model_{O+F}$ ) and a  
4 | dataset of operational measurements only ( $model_O$ ). The continuity of field-based snowpack  
5 | measurements, as provided within this study, is essential given the assumption of non-  
6 | stationarity from hydroclimatic change (Milly et al., 2008) and indications of more extreme  
7 | conditions (IPCC, 2007). This examination of two very different snow years may represent  
8 | the bounds of extremes and possibly the limitations due to non-stationarity. Continued field  
9 | measurements of the snowpack will aid advancement of remote sensing and modeling  
10 | applications, but more importantly continue to provide ground-truth observations for  
11 | evaluating the complexities and uncertainties of the changing earth system.

**Deleted:** strongly

**Deleted:** drive

**Deleted:** field-based and operational

12

### 13 **Acknowledgements**

14 This research was supported by the NASA Terrestrial Hydrology Program (Grant #  
15 NNX11AQ66G). Support for publishing was provided from the Colorado State University  
16 Libraries Open Access Research and Scholarship Fund. Thanks to James Meiman for  
17 discussions on basin scale snow variability. We acknowledge the contributions of the Natural  
18 Resources Conservation Service for the collection of SNOTEL and snow course  
19 measurements. Those who helped with field data collection are acknowledged with thanks.  
20 We would like to thank Adam Winstral of ARS and an anonymous review for their  
21 constructive comments.

22

23

## 1 **References**

- 2 Akaike, H.: A new look at the statistical model identification, *IEEE T. Automat. Contr.*, 19,  
3 716-723, 1974.
- 4 Anderton, S. P., White S. M, and Alvera B.: Evaluation of spatial variability in snow water  
5 equivalent for a high mountain catchment, *Hydrol. Process.*, 18, 435-453, 2004.
- 6 Bales, R. C., Molotch N. P., Painter T. H., Dettinger M. D., Rice R., and Dozier J.: Mountain  
7 hydrology of the western United States, *Water Resour. Res.*, 42, W08432,  
8 doi:10.1029/2005WR004387, 2006.
- 9 Barry, R. G., *Mountain Weather and Climate*, 3rd ed., Cambridge University Press,  
10 Cambridge, 1998.
- 11 Berk, K. N.: Comparing Subset Regression Procedures, *Technometrics*, 20, 1-6, 1978.
- 12 Blöschl, G.: Scaling issues in snow hydrology, *Hydrol. Process.*, 13, 2149-2175. 1999.
- 13 Blöschl, G., Kirnbauer, R., and Gutknecht D.: Distributed Snowmelt Simulations in an Alpine  
14 Catchment 1. Model Evaluation on the Basis of Snow Cover Patterns, *Water Resour. Res.*, 27,  
15 3171-3179, 1991.
- 16 Clow, D. W.: Changes in the Timing of Snowmelt and Streamflow in Colorado: A Response  
17 to Recent Warming, *J. Climate*, 23, 2293-2306, 2010.
- 18 Daly, S.F., Davis R., Ochs E., and Pangburn T.: An approach to spatially distributed snow  
19 modeling of the Sacramento and San Joaquin basins, California, *Hydrol. Process.*, 14, 3257-  
20 3271, 2000.
- 21 Dingman, S.L.: *Elevation: A major influence on the hydrology of New Hampshire and*  
22 *Vermont, USA*, *Hydrol. Sci. Bull.*, 26, 399-413, 1981.
- 23 Doesken, N.J., and Judson A.: *The Snow Booklet: A Guide to the Science, Climatology, and*  
24 *Measurement of Snow in the United States*, Dep. of Atmos. Sci., Colo. State Univ., Fort  
25 Collins, CO., 1996.
- 26 Dressler, K., Fassnacht, S. R., and Bales, R. C.: A Comparison of Snow Telemetry and Snow  
27 Course Measurements in the Colorado River Basin, *J. Hydrometeorol.*, 7, 705-712, 2006.
- 28 Elder, K., Dozier, J., and Michaelson, J.: Snow accumulation and distribution in an Alpine  
29 watershed, *Water Resour. Res.*, 27, 1541-1552, 1991.

- 1 [Elder, K., Michaelsen, J., Dozer, J.: Small basin modelling of snow water equivalence using](#)  
2 [binary regression tree methods, Proc. Symp. on Biogeochemistry of Seasonally Snow-](#)  
3 [Covered Catchments, Boulder, CO, IAHS-AIHS and IUGG XX General Assembly, IAHS](#)  
4 [Publication 228, 129-139, 2005.](#)
- 5 Elder, K., Rosenthal, W., and Davis, R. E.: Estimating the spatial distribution of snow water  
6 equivalence in a montane watershed, *Hydrol. Process.*, 12, 1793-1808, 1998.
- 7 Erickson, T. A., Williams, M. W., and Winstral, A.: Persistence of topographic controls on  
8 the spatial distribution of snow in rugged mountain terrain, Colorado, United States, *Water*  
9 *Resour. Res.*, 41, W04014, doi:10.1029/2003WR002973, 2005.
- 10 Erxleben, J., Elder, K., and Davis, R.: Comparison of spatial interpolation methods for  
11 estimating snow distribution in the Colorado Rocky Mountains, *Hydrol. Process.*, 16, 3627-  
12 3649, 2002.
- 13 ESRI: ArcGIS Desktop: Release 10. Redlands, CA: Environmental Systems Research  
14 Institute, 2011.
- 15 Fassnacht, S. R., Dressler, K. A., and Bales, R. C.: Physiographic parameters as indicators of  
16 snowpack state for the Colorado River Basin, Proceedings of 58th Eastern Snow Conference,  
17 Ottawa, Ontario, Canada, May 2001.
- 18 Fassnacht, S. R., Dressler, K. A., and Bales, R. C.: Snow water equivalent interpolation for  
19 the Colorado River Basin from snow telemetry (SNOTEL) data. *Water Resour. Res.*, 39,  
20 1208-1218, 2003.
- 21 Fassnacht, S. R., Dressler, K. A., Hulstrand, D. M., Bales, R. C., and Patterson, G.: Temporal  
22 Inconsistencies in Coarse-Scale Snow Water Equivalent Patterns: Colorado River Basin Snow  
23 Telemetry-Topography Regressions, *Pirineos*, 167, 167-186, 2012.
- 24 Fassnacht, S. R., Heun, C. M., López-Moreno, J. I., and Latron, J. B. P.: Variability of Snow  
25 Density Measurements in the Rio Esera Valley, Pyrenees Mountains, Spain, *Cuadernos de*  
26 *Investigación Geográfica (Journal of Geographical Research)*, 36, 59-72, 2010.
- 27 Fassnacht, S. R., Skordahl, M. E., and Derry, J. E.: Variability at Colorado Operational Snow  
28 Measurement Sites, Snowcourse Stations at Collocated Snow Telemetry Stations,  
29 Proceedings of 65th Eastern Snow Conference, Fairlee, Vermont, USA, May 2008.

1 Harshburger, B. J., Humes, K. S., Walden, V. P., Blandford, T. R., Moore, B. C., and  
2 Dezzani, R. J.: Spatial interpolation of snow water equivalency using surface observations  
3 and remotely sensed images of snow-covered area, *Hydrol. Process.*, 24, 1285-1295. 2010.

4 [Intergovernmental Panel on Climate Change \(IPCC\): Climate Change 2007: The Physical](#)  
5 [Science Basis: Contribution of Working Group I to the Fourth Assessment Report of the](#)  
6 [IPCC](#), edited by Solomon, S., Qin, D., Manning, M., Chen, Z., Marquis, M., Averyt, K. B.,  
7 Tignor, M., and Miller, H. L., Cambridge Univ. Press, Cambridge, U.K., 2007.

8 Jasinski, M., Stoll, J., Carabajal, C., and Harding, D.: Feasibility of Estimating Snow Depth in  
9 Complex Terrain Using Satellite Lidar Altimetry, Eastern Snow Conference, Claryville, NY,  
10 5-12 June 2012, 2012.

11 [Jepsen, S. M., Moltch, N. P., Williams, M. W., Rittger, K. E., and Sickman, J. O.: Interannual](#)  
12 [variability of snowmelt in the Sierra Nevada and Rocky Mountains, United States: Examples](#)  
13 [from two alpine watersheds, \*Water Resour. Res.\*, 48, W02529, doi:10.1029/2011WR011006,](#)  
14 [2012.](#)

15 Jonas, T., Marty, C., and Magnusson, J.: Estimating the snow water equivalent from snow  
16 depth measurements in the Swiss Alps, *J. Hydrol.*, 378, 161-167, 2009.

17 Jost, G., Weiler, M., Gluns, D. R., and Alila, Y.: The influence of forest and topography on  
18 snow accumulation and melt at the watershed-scale, *J. Hydrol.*, 347, 101-115, 2007.

19 Kimerling, A.J., Buckley, A. R., Muehrcke, P. C., and Muehrcke, J. E.: *Map Use: Reading*  
20 *Analysis Interpretation*, Seventh Edition. ESRI Press Academic, Redlands, California, 2011.

21 Kutner, M. H., Nachtsheim, C. J., Neter, J., and Li, W.: *Applied Linear Statistical Models*,  
22 Fifth Edition. McGraw-Hill/Irwin, New York, NY, 2005.

23 Lapen, D. R. and Martz, L. W.: An investigation of the spatial association between snow  
24 depth and topography in a prairie agricultural landscape using digital terrain analysis, *J.*  
25 *Hydrol.*, 184, 277-298, 1996.

26 Liston, G. E. and Sturm, M.: A snow-transport model for complex terrain, *J. Glaciol.*, 44,  
27 498-516, 1998.

28 Logan, L. A.: Basin-wide water equivalent estimation from snowpack depth measurements,  
29 *IAHS-AISH P.*, 107, 864-884, 1973.

**Deleted:** Homer, C., Dewitz, J., Fry, J., Coan, M., Hossain, N., Larson, C., Herold, N., McKerrow, A., VanDriel, J. N., and Wickham, J.: Completion of 2001 National Land Cover Database for the Conterminous United States. *Photogramm. Eng. Rem. S.*, 73, 337-341, 2007. ¶

- 1 López-Moreno, J. I., Fassnacht S. R., Beguería, S., and Latron, J. B. P.: Variability of snow  
2 depth at the plot scale: implications for mean depth estimation and sampling strategies, *The*  
3 *Cryosphere*, 5, 617-629, 2011.
- 4 López-Moreno, J. I., Fassnacht, S. R., Heath, J. T., Musselman, K. N., Revuelto, J., Latron, J.,  
5 Morán-Tejeda, E., and Jonas, T.: Small scale spatial variability of snow density and depth  
6 over complex alpine terrain: Implications for estimating snow water equivalent, *Adv. Water*  
7 *Resour.*, 55, 40-52, 2013.
- 8 López-Moreno, J. I. and Nogués-Bravo, D.: Interpolating local snow depth data: an evaluation  
9 of methods, *Hydrol. Process.*, 20, 2217-2231, 2006.
- 10 Mallows, C. L.: Some Comments on  $C_p$ , *Technometrics*, 15, 661-675, 1973.
- 11 McClung, D. and Schaerer, P.: *The Avalanche Handbook*, Third Edition, The Mountaineers  
12 Books, Seattle, WA, 2006.
- 13 Milly P. C. D., Betancourt, J., Falkenmark, M., Hirsch, R. M., Zbigniew, W. K., Lettenmaier.,  
14 D. P., and Stouffer, R. J.: Stationarity Is Dead: Whither Water Management?, *Science*, 319,  
15 573-574, 2008.
- 16 Mizukami, N. and Perica, S.: Spatiotemporal characteristics of snowpack density in the  
17 mountainous regions of the Western United States, *J. Hydrometeorol.*, 9, 1416-1426, 2008.
- 18 Molotch, N. P. and Bales, R. C.: Scaling snow observations from the point to the grid  
19 element: Implications for observation network design, *Water Resour. Res.*, 41, W11421,  
20 doi:10.1029/2005WR004229, 2005.
- 21 Molotch, N. P., Colee, M. T., Bales, R. C., and Dozier, J.: Estimating the spatial distribution  
22 of snow water equivalent in an alpine basin using binary regression tree models: The impact  
23 of digital elevation data and independent variable selection, *Hydrol. Process.*, 19, 1459-1479,  
24 2005.
- 25 [Montesi, J., Elder, K., Schmidt, R. A., and Davis, R. E.: Sublimation of Intercepted Snow](#)  
26 [within a Subalpine Forest Canopy at Two Elevations, \*J. Hydrometeorol.\*, 5, 763-773, 2004.](#)
- 27 Pomeroy, J. W. and Gray, D. M.: *Snow Accumulation, Relocation and Management*. National  
28 Hydrology Research Institute Science Report No. 7, 1995.

- 1 R Development Core Team: R: A language and environment for statistical computing. R  
2 Foundation for Statistical Computing, Vienna, Austria, ISBN 3-900051-07-0, URL  
3 <http://www.R-project.org/>, 2012.
- 4 Richer, E. E., Kampf, S. K., Fassnacht, S. R., and Moore, C. C.: Spatiotemporal index for  
5 analyzing controls on snow climatology: Application in the Colorado Front Range, *Phys.*  
6 *Geogr.*, **34**, 85-107, doi: 10.1080/02723646.2013.787578, 2013.
- 7 Stewart, I. T.: Changes in snowpack and snowmelt runoff for key mountain regions, *Hydrol.*  
8 *Process.*, **23**, 78-94, 2009
- 9 Sturm, M., Taras, B., Liston, G. E., Derksen, C., Jonas, T., and Lea, J.: Estimating Snow  
10 Water Equivalent Using Snow Depth Data and Climate Classes, *J. Hydrometeorol.*, **11**, 1380-  
11 1394, 2010.
- 12 Viviroli, D., Archer, D. R., Buytaert, W., Fowler, H. J., Greenwood, G. B., Hamlet, A. F.,  
13 Huang, Y., Koboltschnig, G., Litaor, M. I., López-Moreno, J. I., Lorentz, S., Schädler, B.,  
14 Schreier, H., Schwaiger, K., Vuille, M., and Woods, R.: Climate change and mountain water  
15 resources: overview and recommendations for research, management and policy, *Hydrol.*  
16 *Earth Syst. Sc.*, **15**, 471-504, 2011.
- 17 Viviroli, D., Weingartner, R., and Messerli, B.: Assessing the Hydrological Significance of  
18 the World's Mountains, *Mt. Res. Dev.*, **23**, 32-40, 2003.
- 19 Washichak J. N. and McAndrew, D. W.: Snow Measurement Accuracy in High Density Snow  
20 Course Network in Colorado, Proceedings of the 35th Western Snow Conference, Boise,  
21 Idaho, USA, April 1967.
- 22 Winstral, A., Elder, K., and Davis, R. E.: Spatial Snow Modeling of Wind-Redistributed  
23 Snow Using Terrain-Based Parameters, *J. Hydrometeorol.*, **3**, 524-538, 2002.

Deleted: , in press

1 Table 1. Historic snow course bivariate correlations between snow density, SWE, snow depth,  
 2 Julian day, elevation, UTM Northing, and UTM Easting and snow density model calibration  
 3 and validation performance statistics. Performance statistics for snow water equivalent based  
 4 on using modeled snow density and observed snow depth to calculate SWE. Bolded values  
 5 represent statistical significance (p-value < 0.05).

Deleted: 1

	Snow Density	SWE
<i>Bivariate Correlations</i>		
Snow depth	<b>0.39</b>	<b>0.94</b>
Day of year	<b>0.62</b>	<b>0.33</b>
Elevation	<b>0.24</b>	<b>0.60</b>
UTM Northing	-0.03	<b>-0.15</b>
UTM Easting	<b>-0.35</b>	<b>-0.43</b>
<i>Snow Density Model Performance</i>		
NSCE	0.51	0.94
RMSE	45.4 kg m <sup>-3</sup>	44.2 mm
<i>Snow Density Model Validation (RMSE)</i>		
Field measurements (n = 84)	44.7 kg m <sup>-3</sup>	70.3 mm
SNOTEL (n = 121)	62.7 kg m <sup>-3</sup>	56.7 mm
10-fold cross validation	45.4 kg m <sup>-3</sup>	---

6

1 Table 2. Summary statistics ( $\mu$  = mean,  $\sigma$  = standard deviation) for snowpack properties from  
 2 WY 2011 and WY 2012 snow surveys. Statistics calculated separately for manual and  
 3 operational measurements as well as manual measurements in which SWE was estimated  
 4 from the snow density model.

	n	SWE (mm)		$\rho_s$ (kg m <sup>-3</sup> )		$d_s$ (m)	
		$\mu$	$\sigma$	$\mu$	$\sigma$	$\mu$	$\sigma$
<i>WY 2011</i>							
Field measurements	28	356	259	307	37.0	1.10	0.68
Field SWE measurements	11	357	242	309	46.7	1.09	0.60
Estimated SWE	17	356	276	305	30.7	1.10	0.74
SNOTEL measurements	10	577	220	342	38.2	1.66	0.55
Snow course measurements	13	410	239	304	24.5	1.31	0.66
Entire dataset	51	413	256	313	36.9	1.26	0.68
<i>WY 2012</i>							
Field measurements	104	228	106	313	23.9	0.72	0.30
Field SWE measurements	12	264	69	318	44.7	0.85	0.26
Estimated SWE	92	224	109	312	20.0	0.70	0.31
SNOTEL measurements	10	241	113	324	69.9	0.72	0.33
Snow course measurements	13	152	105	285	50.4	0.52	0.32
Entire dataset	127	221	108	311	33.8	0.70	0.31

5

1 Table 3. Bivariate correlations between SWE, snow density, snow depth, and terrain and  
 2 canopy variables for the water year 2011 and 2012 snow surveys. Bolded values represent  
 3 statistical significance ( $p$ -value  $< 0.05$ ).

	WY 2011			WY 2012		
	SWE	$\rho_s$	$d_s$	SWE	$\rho_s$	$d_s$
SWE (mm)	---	---	---	---	---	---
Snow density ( $\text{kg m}^{-3}$ )	<b>0.81</b>	---	---	<b>0.52</b>	---	---
Snow depth (m)	<b>0.99</b>	<b>0.75</b>	---	<b>0.98</b>	<b>0.40</b>	---
Elevation (m)	<b>0.75</b>	<b>0.46</b>	<b>0.77</b>	<b>0.68</b>	<b>0.41</b>	<b>0.67</b>
UTM Easting (m)	<b>-0.69</b>	<b>-0.71</b>	<b>-0.66</b>	<b>-0.38</b>	<b>-0.51</b>	<b>-0.33</b>
UTM Northing (m)	<b>-0.55</b>	-0.36	<b>-0.56</b>	-0.12	-0.02	-0.10
Eastness	-0.13	<b>-0.28</b>	-0.11	0.10	-0.09	0.13
Northness	-0.01	-0.08	0.00	0.06	-0.13	0.08
Canopy cover	-0.20	-0.16	-0.21	<b>-0.22</b>	-0.01	<b>-0.22</b>
Slope ( $^\circ$ )	-0.03	-0.05	-0.01	0.11	0.05	0.13
Curvature 30 ( $\text{m}^{-1}$ )	0.08	0.13	0.08	-0.08	-0.11	-0.04
Curvature 100 ( $\text{m}^{-1}$ )	-0.04	-0.02	-0.02	-0.08	-0.08	-0.06
Solar radiation ( $\text{W m}^{-2}$ )	0.26	0.20	0.25	0.07	<b>0.22</b>	0.04

4  
5

1 Table 4. Partial correlations between SWE and terrain/canopy variables with the effect of  
 2 elevation (z), UTM Easting (x), and UTM Northing (y) removed. Bolded values represent  
 3 statistical significance (p-value < 0.05).

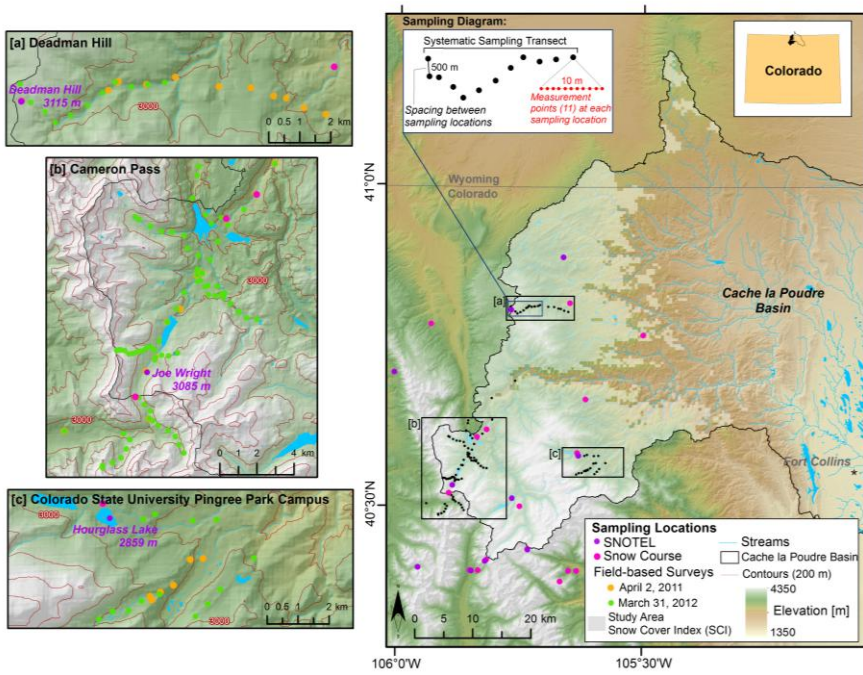
	WY 2011		WY 2012	
	z	z, x, y	z	z, x, y
UTM Easting (m)	<b>-0.74</b>	---	-0.16	---
UTM Northing (m)	<b>-0.38</b>	---	<b>0.16</b>	---
Eastness	-0.07	0.23	0.08	0.10
Northness	0.06	0.18	0.12	0.16
Canopy cover	-0.14	0.06	-0.15	-0.17
Slope (°)	-0.22	<b>-0.28</b>	<b>-0.08</b>	<b>-0.06</b>
Curvature 30 (m <sup>-1</sup> )	-0.07	<b>-0.41</b>	<b>-0.32</b>	<b>-0.31</b>
Curvature 100 (m <sup>-1</sup> )	-0.25	<b>-0.31</b>	<b>-0.36</b>	<b>-0.35</b>
Solar radiation (W m <sup>-2</sup> )	0.02	-0.10	-0.06	-0.13

4

1 Table 5. Beta coefficients (standardized coefficients) and performance statistics for each  
 2 multiple regression model with dependent variable SWE (mm). Each coefficient included in  
 3 the models was statistically significant (p-value < 0.05). Model performance metrics are  
 4 evaluated against the entire dataset (both operational and field) for each year. RMSE and  
 5 MAE statistics are reported as standardized values (value of the statistic divided by the mean  
 6 of the observations).

	model <sub>O+F11</sub>	model <sub>O11</sub>	model <sub>O+F12</sub>	model <sub>O12</sub>	reduced model <sub>O+F12</sub>
<i>n values</i>	51	23	127	23	42
<i>Beta Coefficients</i>					
Elevation (m)	0.52	0.76	0.77	0.98	0.89
UTM Easting (m)	-0.51	-0.45	---	---	---
UTM Northing (m)	-0.23	---	0.13	0.43	0.21
Canopy cover	---	---	-0.14	---	---
Slope <sup>0.5</sup> (°)	-0.12	---	---	---	---
Curvature 30 (m <sup>-1</sup> )	-0.16	-0.21	---	---	-0.36
Curvature 100 (m <sup>-1</sup> )	---	---	-0.28	-0.34	---
<i>Model Performance</i>					
R <sup>2</sup>	0.88	0.84	0.56	0.51	0.70
RMSE (%)	0.21	0.27	0.32	0.34	0.30
MAE (%)	0.16	0.22	0.25	0.26	0.26

7

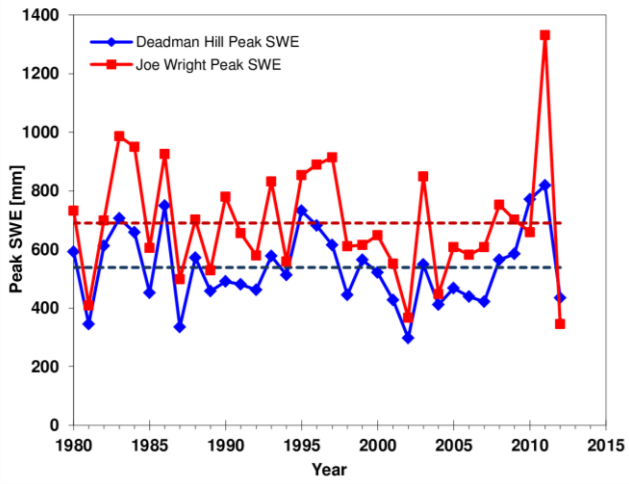


1  
2  
3  
4  
5  
6  
7  
8  
9  
10

Fig. 1. The Cache la Poudre basin located in the northern Front Range of Colorado, U.S.A. The study area is represented by the 50% Snow Cover Index (SCI) which is indicated by the transparent light gray color within the basin. The locations of operational and field-based snow measurements are shown, including a detailed sampling diagram of one systematic field-based sampling transect. The 50% SCI represents the area that was snow covered at least 50% of the time from 2000 – 2010 during early April (Richer et al. 2013). The SCI is calculated from the Moderate Resolution Imaging Spectroradiometer (MODIS)/Terra eight-day snow cover products.

**Deleted:** above the Cache la Poudre River at Canyon Mouth Colorado Division of Water Resources gaging station.  
**Deleted:** and operational

1

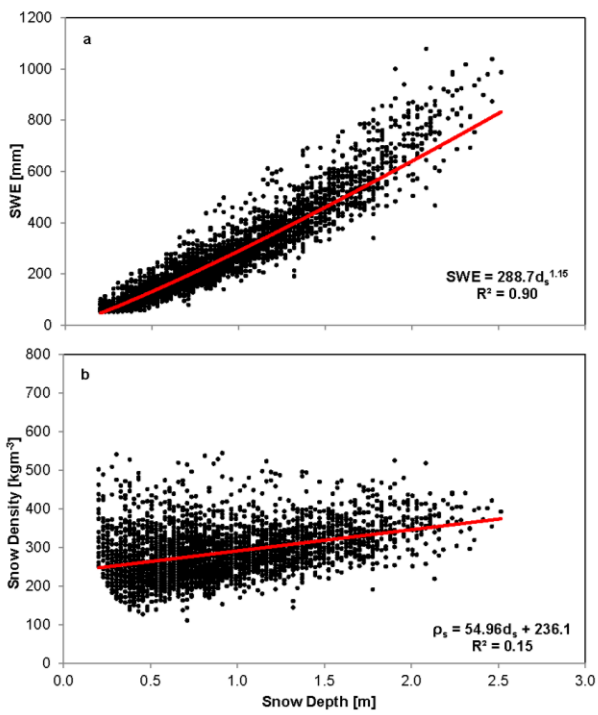


2

3 Fig. 2. Annual peak SWE and mean annual peak SWE (1980 to 2012) for Deadman Hill and  
4 Joe Wright SNOTEL stations.

5

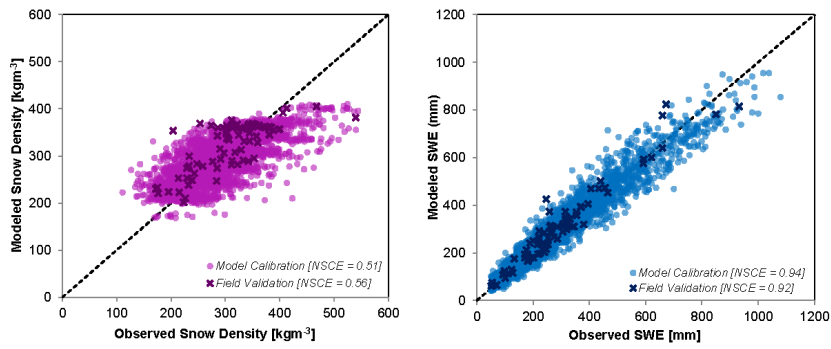
1



2

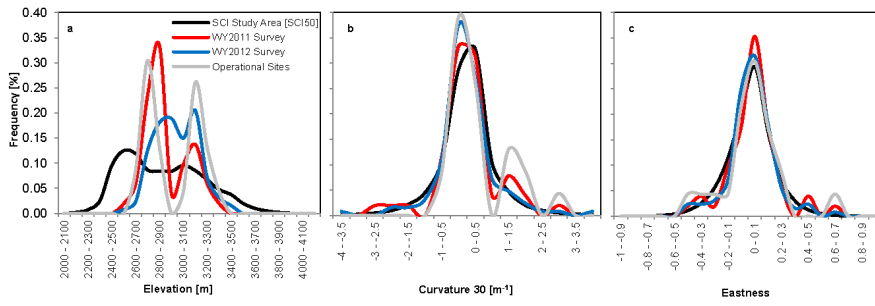
3 Fig. 3. Pairwise relations of SWE and snow density with snow depth from historic snow  
4 course measurements within the study area.

5



1  
 2 Fig. 4. Snow density model versus observed snow density and SWE calibration with historic  
 3 snow course data and validation with independent field data. Modeled SWE is derived from  
 4 modeled snow density and observed snow depth.  
 5

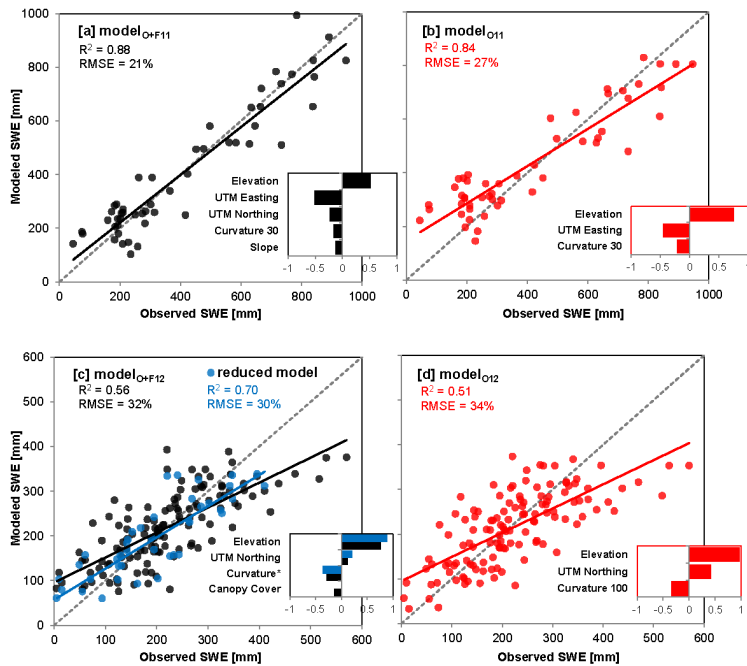
Deleted: 1



1  
 2 Fig. 5. Histograms of terrain variables across the SCI 50 study area compared to variables  
 3 associated with snow measurement locations.

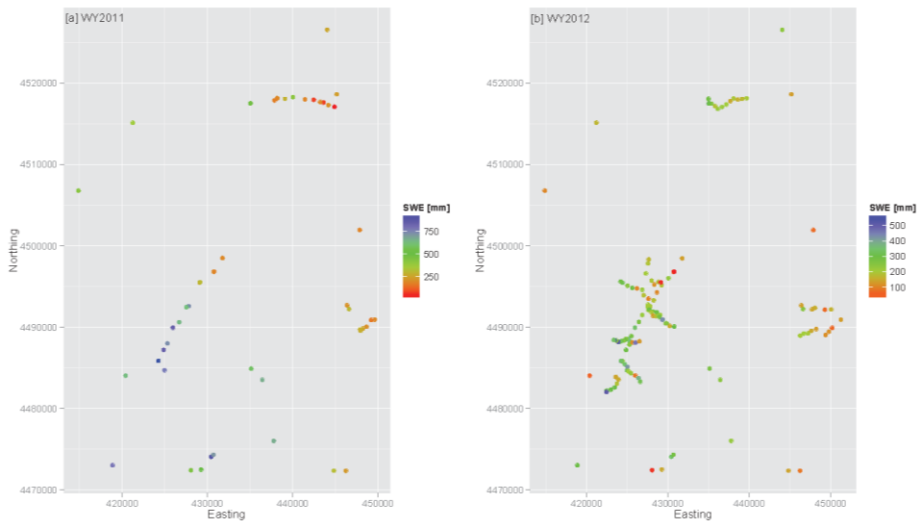
Deleted: and canopy

4



1  
 2 Fig. 6. Scatterplots showing observed versus modeled SWE from model<sub>O+F</sub> (shown in black)  
 3 and model<sub>O</sub> (shown in red) for both WY 2011 and 2012. The observed values used to  
 4 evaluate each model include the combined operational and field-based dataset. The reduced  
 5 model<sub>O+F12</sub> includes only field-based measurement locations also sampled during WY 2011  
 6 (shown in blue). The callout bar graphs show the relative influence of each model coefficient  
 7 (beta coefficients). Curvature\* represents curvature 100 for model<sub>O+F12</sub> and curvature 30 for  
 8 the reduced model.

Deleted: !



1  
 2 Fig. 7. SWE plotted against UTM Northing and UTM Easting for both WY 2011 and WY2012  
 3 snow surveys.